DETECTION OF LOW-METAL MINES USING FREQUENCY-DOMAIN EMI

L. Collins[a], P. Gao[a], J. Moulton[b], L. Makowsky[b], R. Weaver[b], D. Keiswetter[c] and I. J. Won[c]

[a]Department of Electrical and Computer Engineering, Duke University
Box 90291, Durham, NC 27708-0291
Phone: (919) 660-5260, Fax: (919) 660-5293
E-mail: lcollins@ee.duke.edu

[b]Joint UXO Coordination Office, 10221 Burbeck Rd., Ft. Belvoir, VA 22060-5806

[c]Geophex, Ltd., 605 Mercury Street, Raleigh, NC 27603-2343

Abstract Category: UXO Detection

ABSTRACT

Historically, electromagnetic induction (EMI) sensors have been used extensively to locate buried land mines. EMI sensors detect the metal that is present in such mines. However, land mines vary in their construction from metal-cased varieties with a large mass of metal to plastic-cased varieties with minute amounts of metal. Unfortunately, there is often a significant amount of metallic debris (clutter) present in the environment. Consequently, EMI sensors that utilize traditional detection algorithms based solely on the metal content suffer from large false alarm rates. In our previous work, we have developed successful techniques for discriminating between mines and anthropic clutter using a statistical signal processing approach. Currently, the Joint UXO Coordination Office at Ft. Belvoir, VA is sponsoring a series of experiments designed to establish a performance baseline for metallic mine detectors. This baseline will be used to measure the potential improvements in performance offered by advanced signal processing algorithms. In conjunction with this effort, data from low-metal content mines has been gathered using Geophex's GEM-3 sensor and the Schiebel PSS-12.

We have implemented a series of algorithms in order to evaluate the tradeoffs between computational complexity and performance for both sensors. We consider two general classes of algorithms, those which consider only the measured energy and those which process the entire signature. We further divide these two classes into algorithms which operate only on the data measured at a single point, and those measured at various spatial points. In this way, we can quantify the performance of a "baseline", which we consider to be center-point energy-based algorithms. We can also quantify performance gains associated with using the entire signature, as well as incorporation of spatial information. Finally, we consider both ad-hoc procedures and statistically-based Bayesian procedures. In this talk, we will describe these detectors and their performance.

1. INTRODUCTION

Historically, electromagnetic induction (EMI) sensors have been used extensively to locate buried landmines by detecting the metal present in such mines. However, landmines vary in their construction from metal-cased varieties with a large mass of metal to plastic-cased varieties with minute amounts of metal. Unfortunately, there is often a significant amount of metallic debris (clutter) present in the environment. Consequently, EMI sensors that utilize traditional detection algorithms based solely on the metal content suffer from high false alarm rates. To reduce this false alarm problem, we have developed successful techniques for discriminating between mines and anthropic clutter using a statistical signal processing approach applied to time-domain EMI sensors that is based on signal detection theory [1]. The improved performance provided by these algorithms has been validated using data obtained by DARPA; however the metal content of the target set in the DARPA experiment is fairly high and the number of targets is limited.

The Joint UXO Coordination Office at Ft. Belvoir, VA is sponsoring a series of experiments designed to establish a performance baseline for a variety of sensors [2]. This baseline will be used to measure the potential improvements in

performance offered by advanced signal processing algorithms. In conjunction with this effort, data from low-metal content mines has been gathered using a variety of sensors.

One promising approach to mitigating the false alarm problem in landmine detection is to operate the EMI sensor in the frequency-domain utilizing wideband excitation. We have implemented a series of algorithms in order to evaluate performance for the GEM-3 frequency-domain EMI sensor [3]. In the remainder of this paper, we review the non-stationary statistical properties of the noise process (drift) associated with the GEM-3 as well as the mechanism we used to mitigate this drift. Finally, the landmine detection algorithms that were developed are described and their performance is presented and discussed.

2. THE GEM-3 SENSOR

The GEM-3 is a prototype wide-band frequency-domain EMI sensor manufactured by Geophex, Ltd. The GEM-3 uses a pair of concentric, circular coils to transmit a continuous, wideband, digital electromagnetic waveform [3]. The resulting field induces a secondary current in the earth as well as in any buried objects. The set of two transmitter coils has been designed so that they create a magnetic cavity at the center of the two coils. A third receiving coil is placed within the magnetic cavity so that it senses only the weak secondary field returned from the earth and buried objects. The equations governing the response of the GEM-3 are given in [3]. In summary, the measured frequency-domain voltage across the loop is proportional to the magnetic flux and, correspondingly, to the magnetic flux density. The prototype GEM-3 used in this experiment measures the current through a resistor in series with the receiving loop. Measuring the current is equivalent to measuring the voltage across the loop. This current is 90 degrees out of phase with the voltage, and therefore the magnetic flux density. The in-phase and quadrature components at each frequency of interest are obtained by convolving received time-series with a sine time-series (for in-phase) and cosine time-series (for quadrature) at the frequency of interest. The data obtained from the convolution are converted into units called parts-per-million (ppm) defined as

$$ppm = \frac{measured\_data}{calibration\_data} x10^6$$

The calibration data are obtained with the sensor in an approximately “free-field” environment, and are hard-coded into the GEM-3 data acquisition software.

The GEM-3 records in-phase and quadrature data as a function of frequency in ppm. These data are based on an electrical current measurement, as opposed to a magnetic field measurement. Therefore, to convert these measurements to data that are proportional to magnetic field strength, an inverse dependence on the frequency and a 90-degree phase shift must be incorporated. Thus, the following calculations were used for each of the measurements taken:

$$I(f) = -\frac{Q_S(f)}{f}$$
$$Q(f) = \frac{I_S(f)}{f} \quad .$$

Here, f is frequency, $I_s(f)$ and $Q_s(f)$ are the in-phase and quadrature samples reported by the GEM-3, and $I(f)$ and $Q(f)$ are the calculated in-phase and quadrature samples that are proportional to the magnetic field. In the latest version of the GEM-3, this normalization has been built into the data acquisition software.

3. DATA COLLECTION AND ANALYSIS IN THE JUXOCO CALIBRATION LANES

1. Data collection

Details of the data collection plan can be found in [2], however the most salient points are summarized here. A 50 meter by 20 meter plot at Fort A.P. Hill, VA was selected for construction of the test grid, and a calibration area was created in an adjacent 5 meter by 25 meter plot. Initially, all indigenous clutter was removed from the site. Mine targets emplaced in the test grids were predominately “low metal” mines since these are the most challenging targets to detect using EMI sensors. At least one mine of each type used in the main grid, as well as representative samples of clutter, was emplaced in the calibration

area. "Tactical" burial depths were used for the mine targets [6]. Approximately 100 mine targets were buried in the blind grid. The indigenous clutter initially removed from the A.P. Hill site included rusted shrapnel, expended .50 and .30 caliber cases, rusted nails, pieces of wire, small copper pieces and other unidentifiable metal. Samples of the indigenous clutter were re-emplaced in the grids to provide discrete opportunities for false alarms.

The ground truth associated with the calibration area is available; however, the ground truth associated with the main, or blind, test grid is sequestered. A mine or clutter object, when present in a particular grid square, is buried at the center of the 1m x 1m grid square. Algorithm developers provide the output of their algorithms for each grid square or "decision opportunity" to JUXOCO for scoring, thus simplifying the calculation of the detection and false alarm probabilities.

The GEM-3 EMI sensor was programmed to measure responses at 20 frequencies spaced logarithmically between 270 and 23,790 Hz. One meter square data collection templates were constructed for placement at each grid location in both the calibration area and the main test grid to facilitate accurate sensor placement. The templates had a series of marks for use in locating the sensor head at the appropriate positions. Ten spatial positions were measured in each grid point. For grid points in which the GEM-3 response did not overload, these points were located at - 4", - 2", 0", 2", and 4" from the center in both a vertical and a horizontal orientation [2]. Collection points were labeled 1 – 5 from top to bottom and 6 – 10 from left to right (see Figure 1). When the sensor response overloaded, the sensor head was raised 24" above the ground and the spatial samples were taken every 4" as opposed to every 2". Each signature was measured twice.

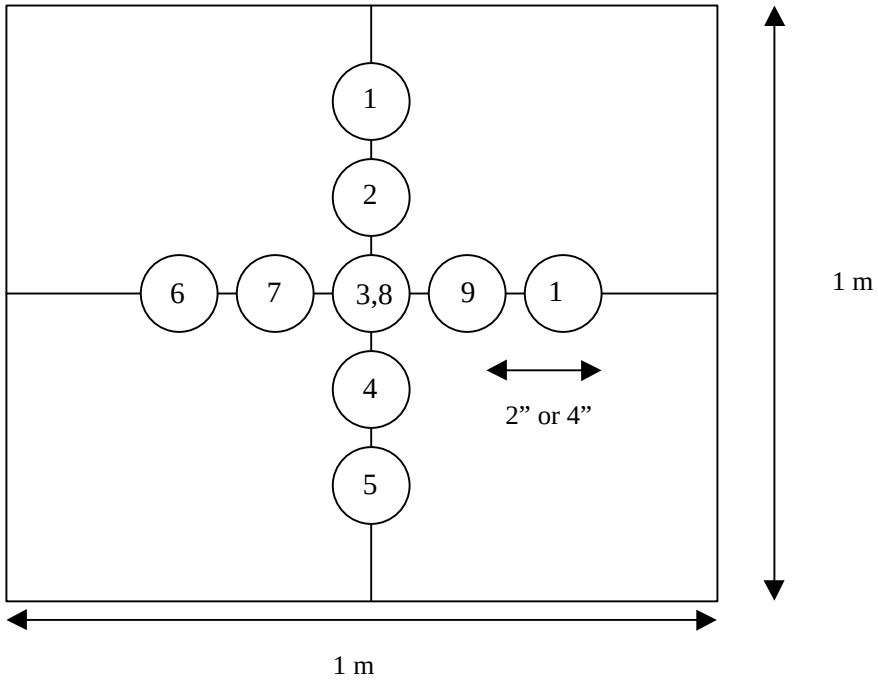

Figure 1. Example of spatial data collection and numbering scheme.

When a mine is present, the response of the sensor consists of the sum of a response due to the mine and a response due to the background. To obtain the response due to the mine alone, it is necessary to determine the response of the sensor to the background alone. We were interested in determining whether this background signature exhibited statistics that were time-invariant, and thus would only need to be characterized once. In order to determine whether or not the statistics of the noise process were stable, we examined the mean and variance of seven sets of data. Each set consisted of 50 consecutive measurements. A total of 350 measurements were made. Figure 2 illustrates the sensor drift using histograms of the 2,370 Hz data measured in each of the free space background scans. The histogram for each scan, denoted backg1 through backg7 respectively, follows the grey-scales listed in the legend. In general, the mean of each scan is increasing with time (scan number), however the mean of backg5 is less than the means of backg3 and backg4. This indicates that the mean, as well as the standard deviation, of the sensor response is not stationary in time.

.

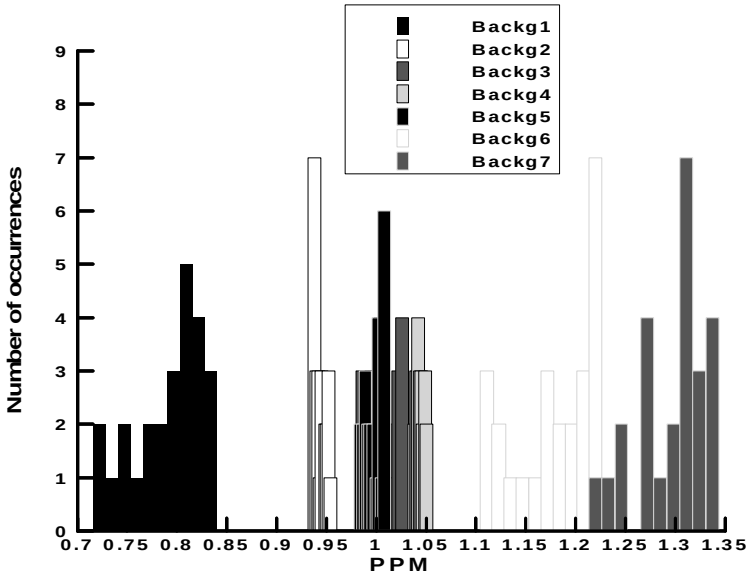

Figure 2. Greyscale-coded histograms of the data obtained at 2,370 Hz during the free space background measurements. The change in both the mean and standard deviation of each data set indicates that the sensor response "drifts", or is not stable over time.

Data was collected in the calibration area four times: on June 9-11, July 6-7, July 27, and September 30, 1998 respectively. Data was measured at each grid point where either a target or clutter had been emplaced. Following the collection of signatures at each of the 10 spatially distributed points corresponding to one grid square, a background measurement was taken at a blank grid point. These "background" measurements were used to track the sensor drift described above. An example of the drift observed on July 7 is shown in Figure 3. The drift observed at the higher frequencies was much greater than that observed previously. This increase in the amount of drift may be due to the relatively hotter temperatures experienced during this data acquisition. Following data collection, the data were hand-corrected for any data drop-outs that occurred as a result of the serial connection between the GEM-3 and the PC controller. Data collection across all ten spatial points associated with a grid square and the subsequent background measurement required, on the average, approximately 10 minutes.

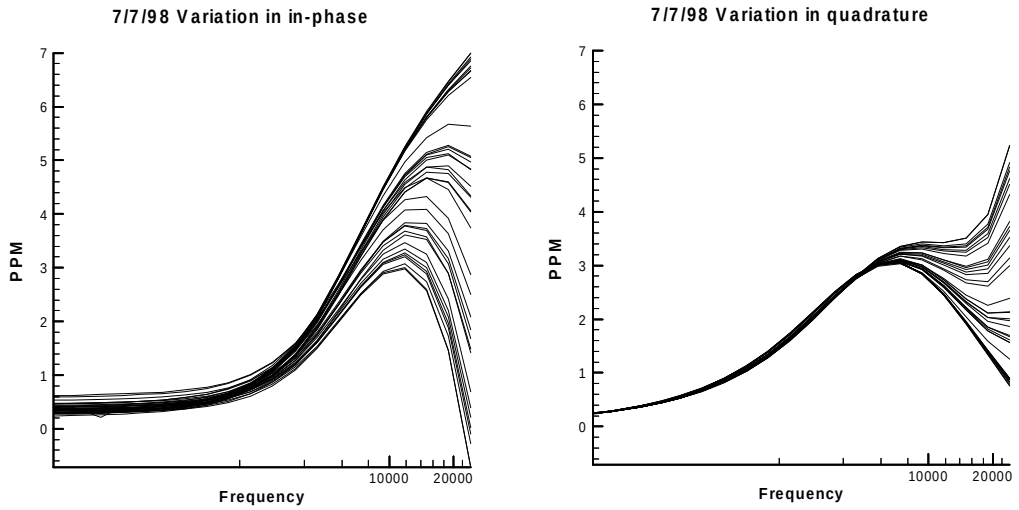

Figure 3. Variation in in-phase and quadrature signals measured on 7/7/98 in the calibration area.

Figure 4 also illustrates the sensor drift characteristics. The measured in-phase component for four of the twenty frequencies is plotted as a function of time, or sample. There is clearly some correlation in the drift across frequency, but the pattern of drift is not identical across frequency.

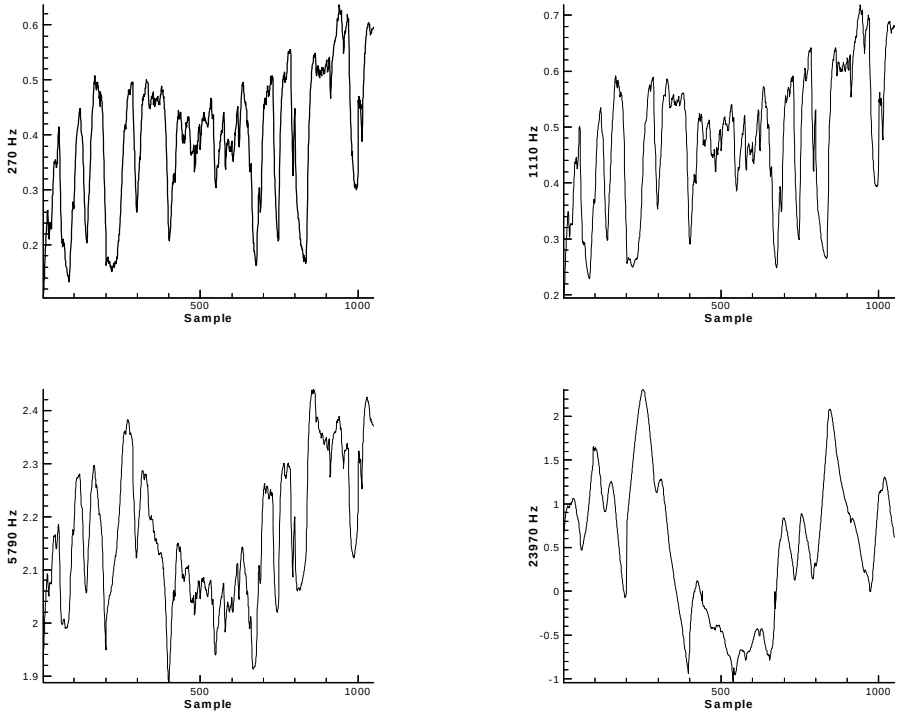

Figure 4. Variation in in-phase signals over time, or sample, measured on 7/7/98 in the calibration area. Variation as a function of time shown for the 270 Hz, 1110 Hz, 5790 Hz, and 23970 Hz in-phase components.

2. Background correction

Several approaches for background correction were analyzed. The performance of the background correction algorithms was analyzed by performing one measurement in which a background was taken between every spatial measurement, *i.e.* the order of measurements was Background 1 – Spatial position 1 – Background 2 - Spatial position 2 - … - Background 10 –

Spatial position 10 – Background 11. Using this approach the true background for a particular spatial position could be very accurately estimated from the bordering background measurements. The "actual" background-corrected signatures could then be compared to those obtained using the various correction methods. The methods that were investigated included using Background 1, Background 11, the average of Background 1 and 11, and linear prediction using Backgrounds 1 and 11. The results of this analysis indicated that a linear prediction method provided the best approach to background correction [5].

3. Analysis of the effects of spatial and environmental parameters on mine signatures.

The response of the GEM-3 to a low-metal mine changes dramatically between free space and soil [4]. The response also changes as a function of soil moisture. Figure 5 illustrates the change in the signature for a VS50 mine as a function of soil moisture. Conditions at A. P. Hill were wet on 7/7/98 and dry and hot on 7/27/98, and a change in the response (including crossover frequency) is evident. Clearly, it is important to develop signal processing algorithms that are robust to such environmental effects.

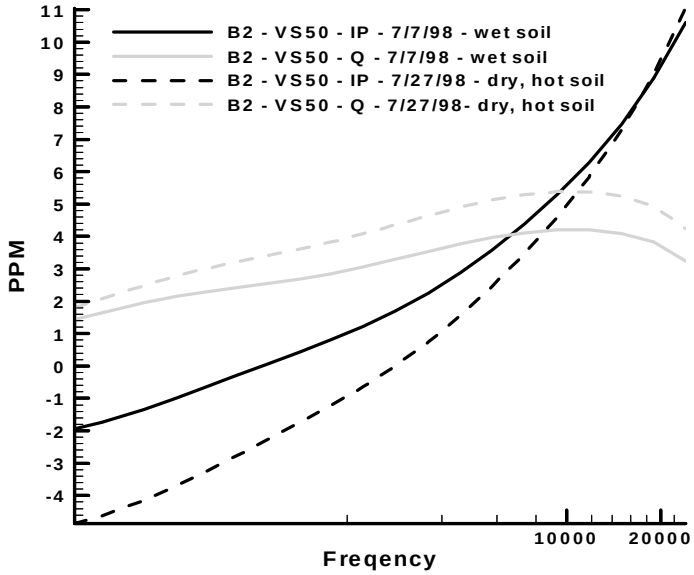

Figure 5. Change in the signature for a VS50 mine as a function of soil moisture

Finally, based on the GEM-3 measurements taken at A. P. Hill, we also observed that the response of the GEM-3 to low-metal objects placed off-axis is not simply a "scaled" version of the on-axis response (see Figure 6). The response does tend to more or less scale with burial depth. Unlike the case of large metallic UXO items where small changes in target-sensor orientation don't dramatically affect the excited modes, in the case of the small metal parts in low metal mines, small changes in orientation can result in dramatic changes in response.

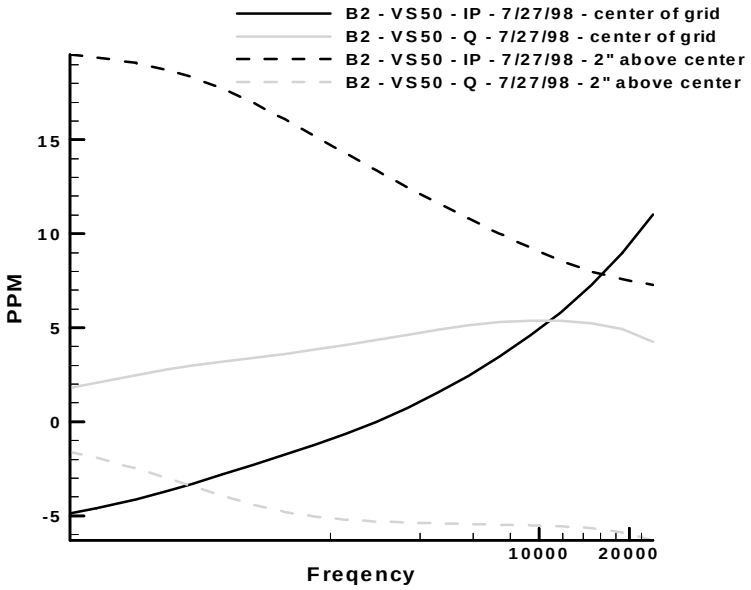

Figure 6. Change in the signature for a VS50 mine as a function of spatial position

4. Discussion of results

The main goal for the data collection in the calibration lanes was to use the GEM-3 sensor to collect data from a sample of mines and clutter in order to develop statistics for algorithm development. The data was also used to (1) characterize the variability of the signatures, and (2) to develop a data-collection/data-processing technique to compensate for sensor drift. The results can be summarized as:

- The sensor experiences some drift in its response, and the drift is more substantial on hot days. Based on this, we felt it was necessary to gather a "background" signature after every grid point measurement.
- A linear prediction using the background signature measured prior to data acquisition and immediately after data acquisition at a grid point provided the best "drift correction".
- Measured signatures changed across days due. These changes may have been due to differences in soil moisture or temperature.
- The spatial variability in signatures was greater in low-metal targets than high-metal targets, and could not be described by a simple scaling.

4. DATA COLLECTION AND ANALYSIS IN THE JUXOCO MAIN GRID

1. Experiment description

Hand-held mine detector experiments were conducted in the main grid between July and October 1998 at Fort A. P. Hill. The test site and preparation are described in detail in [2], and the data collection mechanisms are described in Section 3. The main test grid was established consisting of approximately 100 targets, and an unknown number of clutter objects and blank squares. The main grid consisted of 20 lanes, labeled A – T, each 49 meters long and 1 meter wide. At each grid point, the data and time of the collection were recorded. Background measurements were taken at one of four grid squares: E11, E39, O11 and O39. These squares were set aside as known "blanks" by JUXOCO. The closest "blank" square was used as the background for each grid square while the measurements were taken in the lanes. A background measurement was taken after each grid square was measured.

2. Algorithm development and performance evaluation

We consider two classes of algorithms: those which are based solely on the energy measured at a particular point, and those which process the measured signature. We further divide these two classes into algorithms which operate only on the data

measured at the center of the grid, and those measured at the various spatial points. In this way, we can quantify the performance of a "baseline", which we consider to be center-point energy-based algorithms. We can also quantify performance gains associated with using the entire frequency-domain signature, as well as incorporation of spatial information. The data from the calibration lanes could be used to develop the parameters required for a generalized likelihood ratio test (GLRT) [7]. The GLRT is:

$$\Omega(\mathbf{x}) = \frac{f(\mathbf{x} / \overline{\Theta}, H_1)}{f(\mathbf{x} / \overline{\Gamma}, H_0)}$$

$$\overline{\Theta}, \overline{\Gamma} = \text{ MLE of } \Theta \text{ and } \Gamma$$

where **x** is the measured data (frequency domain or spatial), Θ and Γ are the unknown parameters associated with H_1 and H_0, respectively. H_1 is the hypothesis that a target is present, and H_0 is the hypothesis no target present, *i.e*. clutter or noise only. We assume, based on field measurements, that the pdfs, $f(\mathbf{x}|\Theta,H_1)$ and $f(\mathbf{x}|\Gamma,H_0)$, can be modeled as normal distributions and that the unknown parameters can be associated with a particular mine type, in the case of H_1, or a clutter class (large versus small versus "blank"), in the case of H_0. Thus, the decision statistic becomes

$$\Omega(x_1, x_2, \text{K } x_N) = \frac{\frac{1}{M}\sum_{j=1}^{M} f(x_1, x_2, \text{K } x_N / t_j, H_1)}{\sum_{j=1}^{K} f(x_1, x_2, \text{K } x_N / c_j, H_0) \Pr(c_j)}$$

where *t* corresponds to the various targets and *c* to the various clutter classes, $\Pr(c_j)$ is the *a priori* probability that the *j*th type of clutter class is present. We assume that each of the *M* mines is equally likely. Figure 7 shows the performance of four detectors. The ground truth for the main grid has not been released by JUXOCO, thus the performance curves were produced at JUXOCO. One of the detectors presented is a GLRT operating on the frequency-domain EMI data measured at the center of each grid point, one is a GLRT operating on the energy data measured at the ten spatial positions, and one is an energy detector using the energy data from the center of each grid point. The final algorithm is a GLRT that operated on the output of the two GLRTs mentioned above (frequency domain signature at center point and spatial energy data). Thus, this algorithm performs a sort of "fusion" of the spatial and frequency domain data. However, it is not the optimal approach. An improved algorithm that utilizes all of the frequency domain data as a function of space is still under development.

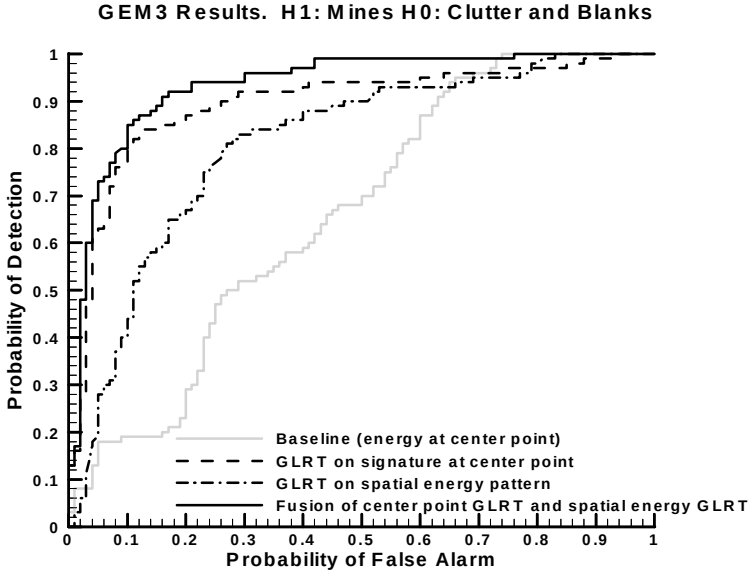

Figure 7. Performance of the baseline algorithm and three GLRT-based algorithms. Performance is computed by JUXOCO.

The improvement in false alarm rates between the various GLRT-based algorithms and the baseline algorithms can be computed by fixing the probability of detection and calculating the ratio between the false alarm probabilities of the various algorithms to that associated with the baseline algorithm. These false alarm rate improvements are summarized in Table I.

Clearly, substantial improvements in false alarm probabilities can be obtained at each of the detection probabilities considered.

Probability of Detection	Fusion of Signature-based GLRT and Energy-based Spatial GLRT	Signature-based GLRT at center point	Energy-based spatial GLRT
0.7	10.4	7.4	2.4
0.8	6.3	5.7	2.1
0.9	3.9	2.4	1.3

Table I. Ratio between the false alarm probability of the various algorithms and the false alarm probability of the baseline algorithm at the particular probabilities of detection.

3. Discussion

The main goal for this experiment was to use the GEM-3 sensor to collect data in the main grid at the JUXOCO test site so that this data could be used for algorithm development, and so that we could gauge the performance of our own algorithms. The results can be summarized as:

- The data collected in the main grid (as well as the calibration lanes) has been provided to JUXOCO, and is being disseminated on their web site. In addition, an Excel file listing the data collection parameters for each grid point measured has been provided.
- Preliminary work on algorithm development with this data set is promising. Substantial reductions in the false alarm rate have been obtained by applying a GLRT to the frequency-domain signature obtained at the center point in the grid square. Such algorithms require no modifications to the existing sensor hardware.
- Additional improvements in performance have been obtained by fusing information contained in the pattern of energy across space with the output of the signature-based GLRT.
- A frequency-domain EMI approach coupled with statistical signal processing algorithms shows significant promise for the problem of detecting low-metal mines.

5. ACKNOWLEDGEMENTS

The work is sponsored by Joint UXO Coordination Office via a grant (DAAG55-98-1-0340) administered through the Army Research Office. The authors would like to thank Dr. Lawrence Carin for useful discussions regarding this work, and John Carey, Denis Reidy, David Ferguson, Yingyi Tan, and Stacy Tantum for their help with data collection.

6. REFERENCES

1. L. Collins, P. Gao, and L. Carin, “An Improved Bayesian Decision Theoretic Approach for Land Mine Detection”. IEEE Trans. Geoscience and Remote Sensing, Vol. 37, No. 2, Mar. 1998.
2. “Hand Held Metallic Mine Detector Performance Baselining Collection Plan”, JUXOCO, Ft. Belvoir, VA, December, 1998.
3. I. J. Won, D. A. Keiswetter, and D. R. Hansen, “GEM-3: A Monostatic Broadband Electromagnetic Induction Sensor”. *Jounal of Environmental and Engineering Geophysics*, 2: 53-64, Aug. 1997.
4. L. Collins and P. Gao, “Progress Report I: Signatures of Land Mines in Soil and in Air: Are They Different? What are the Characteristics of the Sensor Noise?”, JUXOCO, Ft. Belvoir, VA, August, 1998.
5. L. Collins, “Final Report, Statistical Signal Processing for Demining: Experimental Validation,” JUXOCO, Ft. Belvoir, VA, December, 1998.
6. FM 20-32, Mine/Countermine Operations Manual, May 1998.
7. H. L. Van Trees, *Detection, Estimation, and Modulation Theory*. New York: John Wiley and Sons, 1968.